Inorganic Chemistry

ARTICLE

pubs.acs.org/IC

pH-Dependent Cu(II) Coordination to Amyloid-β Peptide: Impact of Sequence Alterations, Including the H6R and D7N Familial Mutations.

Bruno Alies,[†] Hélène Eury,[†] Christian Bijani, Lionel Rechignat, Peter Faller, and Christelle Hureau*

CNRS, LCC (Laboratoire de Chimie de Coordination), 205, route de Narbonne, F-31077 Toulouse, France, and Université de Toulouse, UPS, INPT, LCC, F-31077 Toulouse, France

Supporting Information

ABSTRACT: Copper ions have been proposed to intervene in deleterious processes linked to the development of Alzheimer's disease (AD). As a direct consequence, delineating how Cu(II) can be bound to amyloid-β (Aβ) peptide, the amyloidogenic peptide encountered in AD, is of paramount importance. Two different forms of [Cu^{II}(Aβ)] complexes are present near physiological pH, usually noted components **I** and **II**, the nature of which is still widely debated in the literature, especially for **II**. In the present report, the phenomenological pH-dependent study of Cu(II) coordination to Aβ and to ten mutants by EPR, CD, and NMR techniques is described. Although only indirect insights can be obtained from the study of Cu(II) binding to mutated peptides, they reveal very useful for better defining Cu(II) coordination sites in the native Aβ peptide. Four components were identified between pH 6 and 12, namely, components **I**, **II**, **III** and **IV**, in which the predominant Cu(II) equatorial sites are {$-NH_2$, CO (Asp1−Ala2), N_{im} (His6), N_{im} (His13 or His14)}, {$-NH_2$, N^- (Asp1−Ala2), CO (Ala2−Glu3), N_{im}}, {$-NH_2$, N^- (Asp1−Ala2), N^- (Ala2−Glu3), N_{im}} and {$-NH_2$, N^- (Asp1−Ala2), N^- (Ala2−Glu3), N^- (Glu3−Phe4)}, respectively, in line with classical pH-induced deprotonation of the peptide backbone encountered in Cu(II) peptidic complexes formation. The structure proposed for component **II** is discussed with respect to another coordination model reported in the literature, that is, {CO (Ala2−Glu3), 3 N_{im}}. Cu(II) binding to the H6R-Aβ and D7N-Aβ peptides, where the familial H6R and D7N mutations have been linked to early onset of AD, has also been investigated. In case of the H6R mutation, some different structural features (compared to those encountered in the native [Cu^{II}(Aβ)] species) have been evidenced and are anticipated to be important for the aggregating properties of the H6R-Aβ peptide in presence of Cu(II).

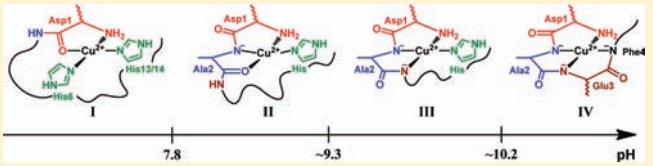

INTRODUCTION

Alzheimer's disease (AD) is the most common cause of dementia in the elderly population with an estimated prevalence of 30 million people worldwide, a number that is expected to quadruple in 40 years.[1] AD is a complex multifactorial neurodegenerative disease in which many genetic and environmental factors are involved. The underlying mechanisms of AD are not clear, but there is evidence and a relatively wide agreement that the so-called amyloid cascade is a key and early event in the development of AD. This hypothesis proposes an increased extracellular accumulation of a peptide, called amyloid-β (Aβ), which leads to its aggregation, first into oligomers, then into protofibrils and last into amyloid plaques, a hallmark of AD. This hypothesis suggests that the mismetabolisms of Aβ and of its precursor protein are initiating events in AD pathogenesis. Formation of Aβ aggregates would further instigate pathological events, including formation of intracellular neurofibrillary tangles (another hallmark of AD), disruption of synaptic connections, ultimately leading to neuronal cells death and dementia.[1−6] Aβ is typically a 39−43 residue polypeptide and consists of a hydrophilic N-terminal domain (1−28) and a C-terminal hydrophobic domain (29−39/43). In vivo, the most prevalent forms of Aβ consist of 40 (Aβ40) and 42 amino acids (Aβ42). The longer form Aβ42 is more prone to aggregation and more toxic to neurons than Aβ40, in agreement with the amyloid cascade hypothesis. Metal ions (Cu, Fe, Zn) have been proposed to play a key role in the development of AD. In vivo, in cello, and in vitro experiments strongly suggest that metal ions and in particular Cu ions are involved in AD. Cu ions can bind to Aβ and modulate its aggregation. Furthermore [Cu(Aβ)] oligomeric forms can catalyze the production of ROS (reactive oxygen species) in presence of physiological reducing agents (e.g., ascorbate), which finally leads to neuronal cells death (for reviews, see refs 7−14).

Copper coordination to the Aβ peptides has been proposed as an important event in the amyloid cascade and deciphering the Cu environment when bound to Aβ peptides is still a burning and controversial topic. At physiological pH, two equatorial binding modes coexist. The one predominant at lower pH is constituted of two equivalent sets of ligands (noted **Ia** and **Ib**), where the terminal $-NH_2$ (from Asp1), the CO from the Asp1−Ala2 peptide bond, a N from imidazole ring of His6 and from His13 (component **Ia**) or from His14 (component **Ib**) are involved.[15−19] The two components have been proposed to be in equilibrium in 1:1 ratio,[15,17] and thus in the following the mixture of **Ia** and **Ib** will be noted component **I**. However, a recent study reported

Received: August 10, 2011
Published: October 06, 2011

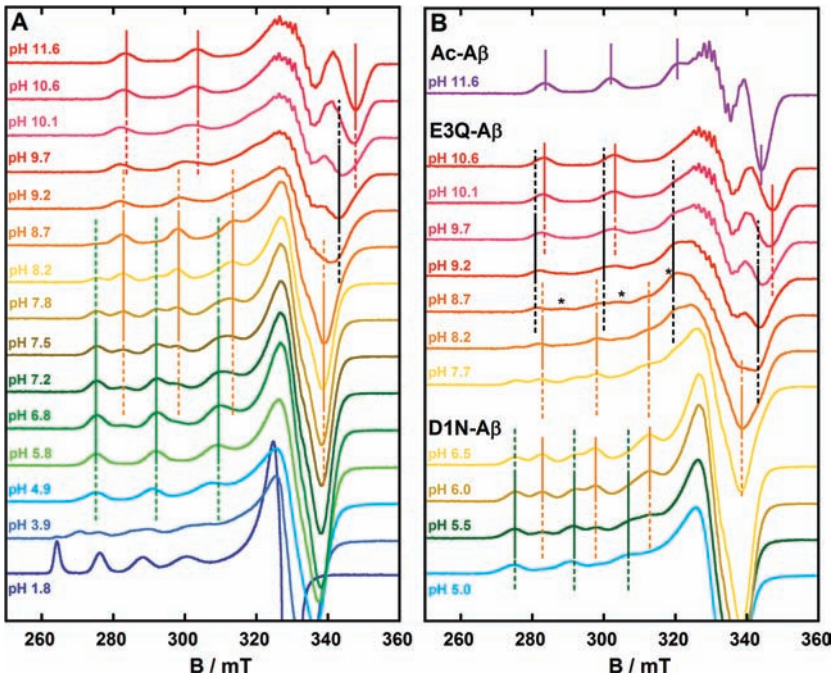

Figure 1. EPR spectra of [Cu^{II}(peptide)] complexes as a function of pH. Panel A: Peptide = Aβ16. Panel B: Peptide = D1N-Aβ, E3Q-Aβ, or Ac-Aβ. Component **I** is designated by green lines, component **II** by orange lines, component **III** by black lines and components **IV** and **IV′** by red and purple lines, respectively. Plain lines indicate pH values where a component is predominant in solution and dotted lines pH range where a component is present in solution but not predominant. [Cu^{II}(peptide)] = 1 mM in D_2O. ν = 9.5 GHz, amplitude modulation = 0.5 mT, microwave power = 20 mW. T = 110 K. * indicates the presence of a minor species, which is not detected in the EPR spectra of other [Cu^{II}(peptide)] species, with $g_{\|}$ = 2.17(8) and $A_{\|}$ = 160 × 10^{-4} cm^{-1} EPR parameters (see Supporting Information for identification of this species).

that a third component, where the two His involved in Cu(II) coordination are the His13 and His14, is also present, this third component (noted **Ic**) being more prone to formation of unstructured aggregates than **Ia** and **Ib**.[20] Regarding the second component (**II**), predominant at higher pH, there are two divergent hypotheses.[19] Mainly on the basis of S-band EPR and HYSCORE data on ^{13}C and ^{15}N isotopically labeled peptides, it was proposed that component **II** is made of the CO group from the Ala2−Glu3 peptide bond and the imidazole rings of the three His.[18] In the second proposition, also deduced from HYSCORE data on ^{13}C and ^{15}N isotopically labeled peptides[15] but from NMR data as well,[16] the $-NH_2$ terminal, the amidyl function N^- from the Asp1−Ala2 peptide bond, the CO from the Ala2−Glu3 peptide bond, and one among the three imidazole rings of His are the functions predominantly involved in equatorial Cu(II) binding. Regarding the apical positions, the debate is still open but involvement of carboxylate groups has been proposed in the literature.[15,16,18]

Here, we report a EPR, CD, and NMR study of Cu(II) binding to the Aβ peptide and to ten mutants that allow discrimination between the two proposed Cu(II) binding models in **II** (see above). Moreover, we describe the pH dependent Cu(II) binding to this series of peptides from pH 4 to 12. While such a pH range is not biologically pertinent, study performed outside the physiological range do help disentangling Cu(II) coordination features around physiological pH. Indeed, the Cu(II) peptidic species are generally obtained from each other by successive deprotonation (protonation) of the peptide when the pH is increased (decreased).[21,22] Moreover, such a wide study is of interest from a chemical point of view since it provides general rules for Cu(II) coordination to peptides. We thus characterized two new components (noted **III** and **IV**) at pH higher than 8.

In this study, the impact on Cu(II) binding properties of the two English (H6R) and Tottori−Japanese (D7N) mutations linked to early onset familial AD were also investigated. In vitro studies of Aβ40 and Aβ42 peptides incorporating either the H6R or the D7N mutations have evidenced that the two mutations alter Aβ assembly at its earliest stages, as well as monomer folding and oligomerization process. Moreover, it was shown that the oligomers of the mutated peptides are more toxic to cultured neuronal cells than the wild type oligomers.[23,24] Trace Cu(II) have not been taken into account in these studies but might influence the aggregation process. Moreover, His6 intervenes in Cu(II) binding and Asp7 is a putative Cu ligand in the wild-type peptide. These are the reasons why it is worth determining how the H6R and the D7N mutations can modify Cu(II) coordination in these rare familial forms of AD. Although beyond the scope of the present phenomenological study, it would be very important to relate the impact of these mutations on the biological properties of the peptides with the difference in the Cu(II) coordination described here.

RESULTS

1. EPR pH-Dependent Study of Cu(II) Binding to Aβ16 Peptides and Mutants. The shorter Aβ16 peptide is used in the present study. Number of previous works have unambiguously shown that it represents the minimum Aβ sequence involved in Cu(II) binding.[25−27] The pH-dependent EPR signature of Cu(II) binding to the Aβ16 peptide is shown in Figure 1 together with spectra of Cu(II) species obtained with the D1N-Aβ and E3Q-Aβ mutants and the N-terminally acetylated (Ac-Aβ) peptide at selected pH values. The EPR signatures of the [Cu^{II}(Aβ)]

dx.doi.org/10.1021/ic201739n |*Inorg. Chem.* 2011, 50, 11192–11201

Table 1. EPR Parameters of Components I−IV and I′−IV′ and of Other [$^{63}Cu^{II}$(peptide)] Complexes for Comparison

	I		II		III		IV				
peptide	$g_{\|}$ [a]	$A_{\|}$ [a]	$g_{\|}$ [a]	$A_{\|}$ [a]	$g_{\|}$ [a]	$A_{\|}$ [a]	$g_{\|}$ [a]	$A_{\|}$ [a]	pK_a(I/II) [b]	pK_a(II/III) [b]	pK_a(III/IV) [b]
human	2.26(2)	184	2.22(6)	161	2.19(1)	194	2.17(3)	203	7.8	9.3	10.2
D1N-Aβ	2.26(3)	180	2.23(0)	160	2.19(1)	194	2.17(4)	201	6.0	9.0	10.3
D7N-Aβ	2.26(2)	184	2.22(7)	160	2.18(8)	194	2.17(4)	197	7.7	9.1	10.6
E3Q-Aβ	2.26(3)	183	2.22(4)	161	2.19(0)	194	2.17(3)	201	7.6	8.5	9.7
E11Q-Aβ	2.26(5)	184	2.22(5)	161	2.18(7)	194	2.17(0)	202	7.5	9.3	10.1
H6A-Aβ	2.26(8)	185	2.22(8)	164			2.17(2)	202	7.3	9.6	
H6R-Aβ	2.26(6)	180	2.22(7)	162			2.17(1)	205	7.2	9.7	
H13A-Aβ	2.26(3)	180	2.23(0)	162			2.17(5)	202	7.5	9.5	10.2
H14A-Aβ	2.26(9)	182	2.22(7)	163			2.17(5)	202	7.5	9.6	10.4
DAHK[28]					2.19	199					
GGGGH[29]			2.23(0)	156	2.19(9)	200	2.17(1)	206			
GGGGG[29]							2.17(1)	206			
	I′		II′		III′		IV′				
Ac-Aβ	2.32(0)	168	2.27(3)	187	2.23(0)	171	2.19(1)	190	5.2	7.5	8.7
GGGTH[30]							2.20	200			

[a] Parallel spin Hamiltonian parameters were obtained directly from the experimental spectra and were calculated from the second and the third hyperfine lines in order to remove second-order effects. $A_{\|}$ parameters are given in 10^{-4} cm^{-1}. [b] pK_a values are roughly estimated from EPR spectra, and with the exception of pK_a(**I**/**II**) that can be estimated accurately, the two others pK_a values are given with an uncertainty of ±0.3 pH unit.

complexes are complicated and generally correspond to the superimposition of several components simultaneously present in solution at a given pH. This is particularly obvious at low pH (near pH 4), at physiological pH where two species coexist (the well-described components **I** and **II**, indicated by green and orange colors in Figure 1, respectively) and at pH near 10. In this latter case, two among the three coexisting components can be well identified: the first one is predominant at pH 8.7 (component **II**) and the other one is predominant above pH 10.6 (that will be noted component **IV**, in red in Figure 1). The third component (noted **III**, in black in Figure 1) is present only as a minor component and is thus difficult to identify. The EPR parameters determined for these four components (**I**−**IV**) are given in Table 1. Regarding the other [Cu^{II}(peptide)] complexes (peptide = Ac-Aβ, D1N-Aβ, E3Q-Aβ, D7N-Aβ, H6A-Aβ, H6R-Aβ, E11Q-Aβ, H13A-Aβ, and H14A-Aβ) studied here (see Figures S1−S3 in the Supporting Information), none of them with the exception of the [Cu^{II}(Ac-Aβ)] has significantly different EPR parameters compared to those of [Cu^{II}(Aβ16)] species (Table 1 and see below for details). Hence, components relative to [Cu^{II}(Ac-Aβ)] will be noted **I**′−**IV**′. Nevertheless, pK_a values corresponding to transition between the various components depend on the nature of the peptide involved in Cu(II) binding (Table 1). Note that the pK_a values are defined as the pH values where the EPR signatures of two components contribute equally to the EPR intensity and thus have been estimated by considering that only two components are simultaneously present in solution.

*a. Components **I** and **II**.* Regarding component **I**, there is now a consensus that the Cu(II) ion lies in an equatorial binding site made of the terminal amine $-NH_2$ group, the imidazole ring of His6, the one of His13 or His14 (in equilibrium) and a carbonyl function,[15−19] the apical position being likely occupied by a carboxylate group.[15,16,18] Species **II**, in which the Cu(II) coordination remains to be elucidated is characterized by EPR parameters that differ from those of component **I** by a concomitant decrease in the $g_{//}$ and $A_{//}$ and are classical for 3N1O or 4N binding site[31] (Table 1). The pK_a of the **I**/**II** transition is approximately 7.8, in line with previous studies.[32,33] In Figure 1, panel B, the EPR pH dependent signatures of Cu(II) bound to the D1N-Aβ mutant is reminded. While the EPR parameters of components **I** from [Cu^{II}(Aβ16)] and [Cu^{II}(D1N-Aβ)] complexes are very similar, the pK_a(**I**/**II**) value is approximately 6.0 in case of the [Cu^{II}-(D1N-Aβ)] complexes, thus significantly lower than that of the [Cu^{II}(Aβ16)] complexes. The D1N mutant was previously studied by the group of Szalai[33] and the decrease in the pK_a(**I**/**II**) was attributed to the breakage of a H-bond network (due to the replacement of the Asp1 anionic carboxylate by a neutral group), which would facilitate the deprotonation of a peptide function during the process leading to component **II**. However, in this pioneer work the peptide function undergoing the deprotonation was not identified.

Regarding the other Cu(II) complexes studied here, none of them with the exception of the [Cu^{II}(Ac-Aβ)] has significantly different EPR parameters compared to [Cu^{II}(Aβ16)]. This strongly suggests that none of the mutated residues is essential for creating the Cu(II) equatorial binding sites and that it can be replaced by an identical residue but located at another position in the peptide sequence. Differences between pK_a(**I**/**II**) values are observed and the most important ones are detected for the [Cu^{II}(H6A-Aβ)] and [Cu^{II}(H6R-Aβ)] complexes, pK_a(**I**/**II**) values being approximately 0.5 pH unit below that of [Cu^{II}(Aβ16)]. This suggests that even if His6 has been proposed to be always equatorially bound to the Cu(II) center in species **I**,[15,17] it can be replaced by either the His13 or His14 thus leading to the equatorial coordination of the His13-His14 diad. In such a coordination environment, geometric constraints accounting for formation of component **II** at a lower pH than in the native [Cu^{II}(Aβ16)] species may be anticipated. On the contrary, the H13A or H14A mutations have only a slight impact on the pK_a(**I**/**II**) values (Table 1), in line with the equilibrium between

dx.doi.org/10.1021/ic201739n |*Inorg. Chem.* 2011, 50, 11192–11201

these two His residues for one equatorial binding position previously proposed.[15,17]

*b. Component **III**.* Component **III** is hardly distinguishable in the pH dependent EPR traces of [Cu^{II}(Aβ16)], being only discernible by the fourth hyperfine feature (black line at B = 343 mT in Figure 1, panel A). Indeed, the three other hyperfine lines are mixed with those of components **II** and **IV** and cannot be well isolated. The reason for such a mixture between components **II**, **III**, and **IV** is likely close pK_a(**II**,**III**) and pK_a(**III**,**IV**) values. To better characterize component **III**, the E3Q mutant is helpful. Indeed, in the [Cu^{II}(E3Q-Aβ)] mutant, component **III** is more easily detected, pK_a(**II**/**III**) and pK_a(**III**/**IV**) values being sufficiently different (estimated to 8.5 and 9.7, respectively). Similar to what was proposed for the D1N-Aβ mutant, we can hypothesize that the Glu3 carboxylate function stabilizes a deprotonable function in its protonated form by H-bond interactions, and that in the [Cu^{II}(E3Q-Aβ)] complex, the H-bond network is broken leading to deprotonation of the function at a lower pK_a(**II**/**III**) value. It is worth noting that mutation of the two other carboxylate functions (leading to D7N and E11Q mutants) do not affect neither the EPR signatures of the corresponding Cu(II) complexes nor their pH dependence compared to [Cu^{II}(Aβ16)]. Parameters of component **III** are close to those observed when the Cu(II) is bound to the ATCUN motif (encountered in peptide with N-terminal XXH- sequence). In such species, the Cu(II) is bound via the $-NH_2$ terminal, the His and the two amidyl functions in between these two residues. For instance, such equatorial Cu(II) coordination is encountered in the N-terminal binding site of the serum albumin having the DAHK sequence.[28] Nevertheless, some minor differences are observed that can be attributed to the formation of three adjacent metallacycles in the ATCUN case, a structural feature that cannot be observed in the present case due to the position of the His compared to the $-NH_2$ group, the closest His residue being far from the terminal amine by 5 amino-acids. Such ATCUN type coordination in component **III** will be further confirmed by NMR studies (see below).

It is also worth noticing that component **III** cannot be detected in the EPR pH-dependent spectra of the [Cu^{II}(H6A-Aβ)] and [Cu^{II}(H6R-Aβ)] complexes. This suggests that His6 is more involved than His13 or His14 in Cu(II) binding in component **III**.

*c. Component **IV**.* The $g_{\|}$ and $A_{\|}$ parameters of component **IV** of [Cu^{II}(peptide)] complexes, with the exception of the [Cu^{II}-(Ac-Aβ)] are characteristic of a 4N equatorial binding mode,[31] where the Cu(II) ion is bound via the terminal $-NH_2$ and three amidyl functions. Indeed, very similar EPR parameters have been reported for the [Cu^{II}(GGGGG)] complex, where the $-NH_2$ is the sole Cu(II) anchoring function and thus where the Cu(II) equatorial site is completed by amidyl groups from adjacent peptide bonds.[29] Such Cu(II) coordination is often encountered in peptidic fragments where other potential ligands are replaced by amidyl functions adjacent to the $-NH_2$ anchoring point when the pH is increased. At high pH, the other possibility is to have a nitrogen atom from the imidazole ring of an His residues as the anchoring point and adjacent amidyl functions that entered is the Cu(II) coordination sphere.[22] This is encountered when the terminal $-NH_2$ is not available for Cu(II) binding, for instance when it is acetylated.[30] In this case, the EPR parameters are different from those observed here in the component **IV** but similar to those observed in component **IV**′ corresponding to complex [Cu^{II}(Ac-Aβ)] at high pH (Figure 1, panel B and Table 1). This agrees with the involvement of the N-terminal amine in equatorial Cu(II) coordination in [Cu^{II}(Aβ16)] at high pH. Note that involvement of the terminal $-NH_2$ function has already been identified by EPR and ENDOR experiments performed on labeled [Cu^{II}(^{15}N-(Asp1)-Aβ16] species.[15] A second consequence is that, Cu(II) center in component **IV** is likely bound by the terminal -NH_2 and the three adjacent amidyl functions while in component **IV**′ by one of the three His and three adjacent amidyl functions, the His residue(s) involved remaining to be identified.

d. [Cu^{II}(Ac-Aβ)] Species. Acetylation of the terminal amine lead to a series of new type of components that can be obtained from component **IV**′ by successive protonation of the amidyl functions, leading to a {$-N_{im}$, $2N^-$, X} equatorial binding site in **III**′ and {$-N_{im}$, N^-, X, Y} in **II**′ and {$-N_{im}$, X, Y, Z} in **I**′, where X, Y, and Z can be either His or CO ligands. Further identification of the exact nature of components **I**′−**IV**′ is beyond the scope of the present paper and is not physiologically relevant for the understanding of Cu(II) coordination to Aβ. Nevertheless, an important point to note is that EPR parameters of components **II**′ and **III**′ are very close to those of components **I** and **II**, respectively and that pK_a(**II**′/**III**′) is also very close to pK_a(**I**/**II**) (Table 1). As a consequence, the pH dependent EPR spectra of [Cu^{II}(Aβ16)] and [Cu^{II}(Ac-Aβ)] complexes will be by chance very similar near physiological pH. This may have led to misinterpretation of comparative EPR data of [Cu^{II}(Aβ16)] and [Cu^{II}(Ac-Aβ)] when recorded only near physiological pH and to the erroneous conclusion that $-NH_2$ is involved in Cu(II) apical position in component **I**.[34]

2. CD pH-Dependent Study of Cu(II) Binding to Aβ16 Peptides and Mutants. EPR is a powerful technique to determine the Cu(II) binding site but reveals information concerning only the equatorial plane. As a consequence, CD can be used to monitor structural modifications that occur outside from the first coordination shell and in apical position. pH-dependent CD spectra of four chosen examples of [Cu^{II}(peptide)] complexes that are representative of the four types of CD signatures obtained in the present study, are shown in Figure 2 ([Cu^{II}(Aβ16)], [Cu^{II}(Ac-Aβ)], [Cu^{II}(H6A-Aβ)], [Cu^{II}(E3Q-Aβ)]).

a. [Cu^{II}(Aβ16)] Type Family. pH dependent CD signatures of this family is shown in Figure 2, panel A. Weak d−d transitions are observed at λ = 670 and 590 nm, which increase in intensity upon increasing pH, reaching a maximum at a pH ∼7.5. A new d−d band at λ = 510 nm is observed when the pH is raised above 7.5. In the UV domain, the intensity of the λ = 315 and 285 nm bands increase from pH approximately 7 and 3, respectively. The former band has been attributed to amide to Cu(II) charge transfer transition (LMCT) while the latter to amine to Cu(II) LMCT. The band detected at λ = 265 nm, which has tentatively been attributed to imidazole to Cu(II) LMCT,[21] increases in intensity from pH approximately 8.5. pH dependent behavior of these features indicates that (i) $-NH_2$ is bound to Cu(II) from pH 3 and remains bound to Cu(II) at any higher pH, (ii) amidyl groups start to bind Cu(II) at pH approximately 7, and (iii) binding of amidyl functions to Cu(II) enhances the molar extinction coefficient of the His to Cu(II) LMCT and of the d−d transitions detected at 265 and 590 nm, respectively. The [Cu^{II}(H13A-Aβ)], [Cu^{II}(H14A-Aβ)] and [Cu^{II}(E11Q-Aβ)] complexes belong to this family (Supporting Information Figures S5 and S6) and thus behave very similarly to the [Cu^{II}(Aβ16)], suggesting that (i) both His13 and His14 are not simultaneously involved in Cu(II) binding in the whole pH range and that

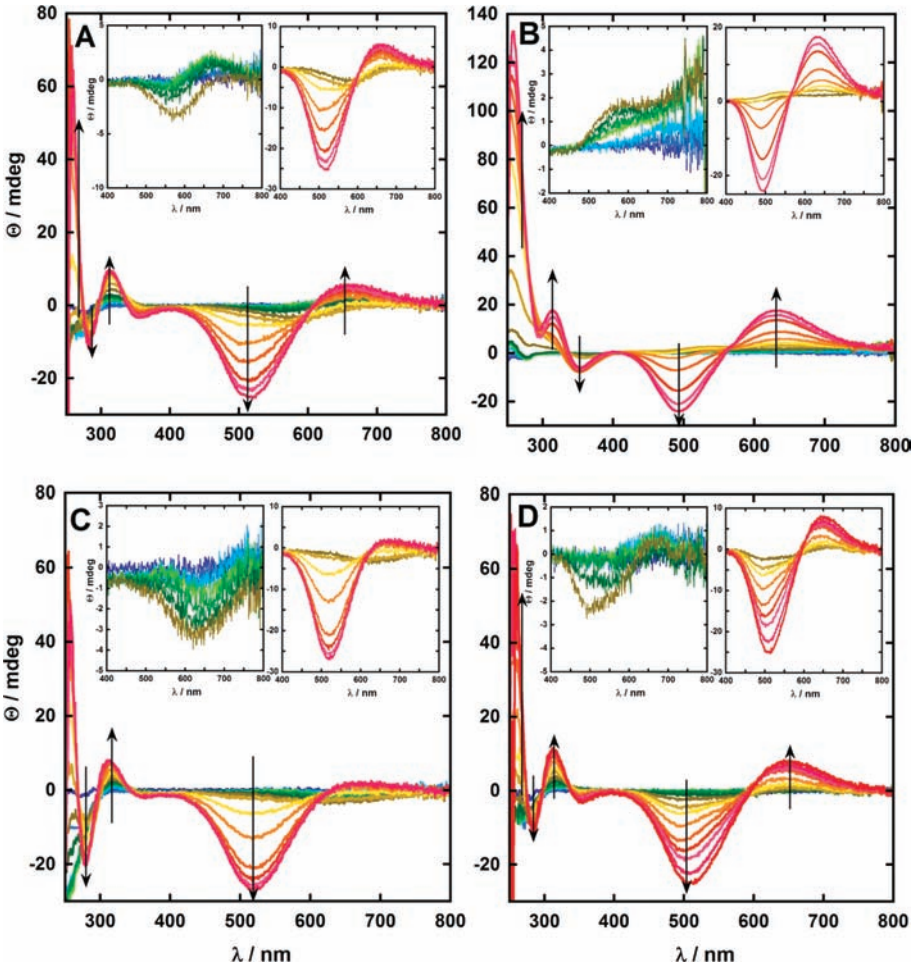

Figure 2. Effect of pH on the CD spectra of [Cu^{II}(peptide)] complexes, from pH approximately 3 (blue line) to pH approximately 12 (red line). Panel A: [Cu^{II}(Aβ16)]. Panel B: [Cu^{II}(Ac-Aβ)]. Panel C: [Cu^{II}(H6A-Aβ)]. Panel D: [Cu^{II}(E3Q-Aβ16)]. Left insets: pH from approximately 3 to approximately 7.5. Right insets: pH from approximately 7.5 to approximately 12. [Cu^{II}(peptide)] = 0.5 mM, ℓ =1 cm, T = 20 °C. Arrows indicate the formation of relevant bands with pH increase. For exact pH values see Supporting Information, Figures S4−S6.

(ii) carboxylate group from Glu11 is not an essential element of Cu(II) binding sites.

b. [Cu^{II}(Ac-Aβ)]. pH-dependent CD signature of [Cu^{II}(Ac-Aβ)] is unique compared to all the other [Cu^{II}(peptide)] complexes studied here (Figure 2, panel B). The continuous increase of bands at λ = 630, 490, 360, 315, and 265 nm is observed when the pH is increased. Two main differences with the [Cu^{II}(Aβ16)] data are the absence of the λ = 285 nm band characteristic of $-NH_2$ to Cu(II) LMCT, in line with acetylation of N-terminal amine and a significantly higher intensity of the λ = 265 nm band, especially at high pH, compared to all the others [Cu^{II}(peptide)] complexes, in agreement with the formation of binding sites centered on His anchoring residue, as previously proposed on the basis of the EPR data analysis.

c. [Cu^{II}(H6A-Aβ)]/[Cu^{II}(H6R-Aβ)] Type Family. These mutations lead to three mains differences in the pH-dependent CD signatures of the [Cu^{II}(peptide)] complexes (Figure 2, panel C and Supporting Information Figure S5), which are (i) a negative d−d band at λ = 630 nm from pH 3 to approximately 7.5; (ii) a more pronounced λ = 285 nm band, and (iii) a λ = 265 nm band, the growth of which begins in the negative part of the CD spectra from pH 3 to approximately 7.5 and the intensity of which remains weaker than in the [Cu^{II}(Aβ16)] type family complexes at higher pH. These modifications may be attributed to the simultaneous involvement of His13 and His14 in Cu(II) binding, a feature that is not detected in the [Cu^{II}(Aβ16)] type family (see above), thus leading to an important reshuffling of the peptide conformation. Sign change in the λ = 265 nm band at pH ~7.5 may also be interpreted as transition between the His13−His14 diad involved in Cu(II) coordination to only one His bound to Cu(II). These CD data are consistent with the EPR data, since it confirms that both His13 and His14 can be simultaneously bound to Cu(II). However, if the EPR traces of both [Cu^{II}(H6A-Aβ)] and [Cu^{II}(H6R-Aβ)] complexes are very close to that of the [Cu^{II}-(Aβ16)], their CD signatures differ significantly, in line with modifications occurring outer from the first coordination shell.

d. [Cu^{II}(E3Q-Aβ)] Type Family. The pH dependent CD spectra of Cu(II) complexes obtained with the triple E3QD7NE11Q mutants and the D1N, E3Q, and D7N mutants (Figure 2, panel D and Supporting Information Figures S4 and S6) are slightly different from that of the [Cu^{II}(Aβ16)] type family by having weaker d−d band intensities up to pH 7.5 (especially in the E3Q and E3QD7NE11Q cases) and then a stronger intensity at λ = 650 nm at higher pH, except for the [Cu^{II}(D1N)] complex that exhibits a weaker intensity. This may reflect involvement of the Glu3 and Asp7 residues in apical Cu(II) binding or an outer first

dx.doi.org/10.1021/ic201739n |*Inorg. Chem.* 2011, 50, 11192–11201

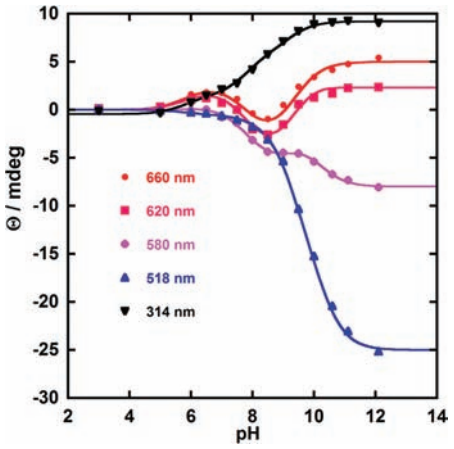

Figure 3. pH-dependent CD absorbance of $[Cu^{II}(A\beta16)]$ complex at λ = 660 (red plain circles), 620 (pink plain squares), 580 nm (purple plain diamonds), 518 nm (blue plain triangles), and 314 nm (black plain triangles). Solid lines are the fits of the curves with pK_a = 5.8, 7.9, 9.3, and 10.3. $[Cu^{II}(A\beta16)]$ = 0.5 mM, ℓ =1 cm, T = 20 °C.

sphere contribution of the Glu3 and Asp7 residues, for instance by creating salt bridge with the Arg5 residue. Furthermore, the CD data obtained here are in line with contribution of the Asp1 residue in Cu(II) apical position even if the different pH-dependent CD signature of the $[Cu^{II}(D1N\text{-}A\beta)]$ complex is mainly due to the low pK_a(**I**/**II**) value.

e. pK_a Determination. Using EPR data it was possible to evaluate the pK_a between various components. As exemplified in Figure 3 in the case of the $[Cu^{II}(A\beta16)]$ complex, this could also be achieved by simulation of the CD data. Simulations of the pH-dependent absorbance curves at several selected wavelengths with a unique set of pK_a values were performed and pK_a(**I**/**II**) = 7.9, pK_a(**II**/**III**) = 9.3, and pK_a(**III**/**IV**) = 10.3 values were found. These results were fully consistent with EPR data suggesting that no significant pH drift occurs upon freezing the EPR samples. In the course of simulation, it appears that more than 3 pK_a values were necessary to correctly fit the curves. More precisely, below pH 6, the intensities of the λ = 620 and 660 nm undergo significant increase. The pK_a value corresponding to transition between component **I** and this newly detected component (noted **0**) is estimated to be 5.8. Regarding the EPR data, it appears that the EPR signature of component **0** is indiscernible to that of component **I**. Hence, a possible explanation is that this pK_a corresponds to the deprotonation of the third Cu(II) unbound His leading to modification of peptide arrangement but not to direct change in the equatorial Cu(II) coordination.

3. NMR Studies of Cu(II) Binding to Aβ in Component III and to H6R-Aβ Mutant in Components I and II. In an attempt to better characterize the new components **III** and **IV**, we used NMR spectroscopy that was previously revealed to be a powerful technique to better disentangle Cu(II) binding to Aβ peptides[16,32] and to others peptides or proteins.[35,36] Indeed the paramagnetism of the Cu(II) ion induces broadening of NMR features that depends on the proximity of the Cu(II) ion. Hence, it is possible to map which residues are affected by the presence of Cu(II) and thus involved in its coordination. ^{13}C NMR spectra of the apo-Aβ and holo-Aβ (0.3 equiv of Cu(II)) recorded at pH 9.8 (where component **III** is predominant) are compared to those of the apo-Aβ and holo-Aβ (0.1 equiv of Cu(II)) at pH 8.7 (Figure 4). Cu(II)-induced broadening of the ^{13}C peaks are weaker at pH 9.8

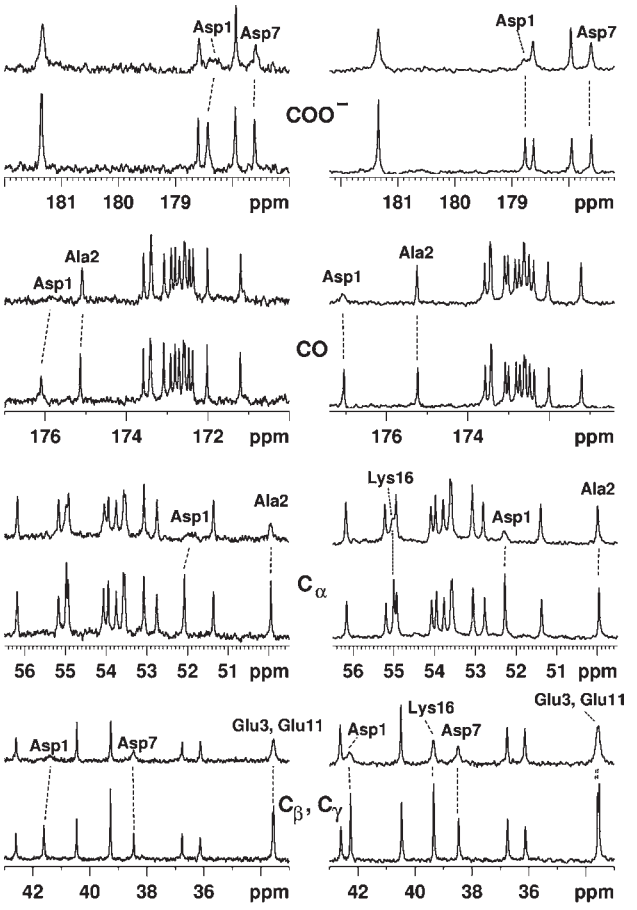

Figure 4. $^{13}C\{^1H\}$ NMR spectra of 10 mM Aβ peptide in D_2O (bottom spectra) and in presence of 0.1 equiv of Cu(II) (top spectra) at pH 8.7 (left) and of 0.3 equiv of Cu(II) (top spectra) at pH 9.8 (right). T = 25 °C, ν = 125.8 MHz. Shift of some peaks is due to slight modification in the pH value induced by Cu(II) addition.

although the Cu(II) stoichiometry is 3-fold higher. Moreover, no new ^{13}C signals, with the exception of the C$_\alpha$ and C$_\beta$ of Lys16, are affected by the Cu(II) addition at pH 9.8 compared to pH 8.7. This behavior is attributed to the formation of a "ATCUN" type Cu(II) binding motif $\{-NH_2, 2N^-, N_{im}\}$ in component **III**. Indeed, it was previously evidenced that in such a coordination site, Cu(II) exchange between peptides is too slow to affect all the peptides present in solution. On the contrary, Cu(II) stays bound to a portion of peptide and then lead to the total disappearance of its NMR signals.[28] Thus in the present case, Cu(II) effect on Aβ NMR peaks corresponding to component **III** is not observable. The broadening effect observed is due to the presence of a small portion of component **II** (in pH-dependent equilibrium with component **III**). As a direct consequence, NMR revealed inappropriate for the study of components **III** and **IV**.

The H6R mutation is a familial mutation that was associated with early onset of AD. Moreover, significant modifications of the pH-dependent CD signature of $[Cu^{II}(H6R\text{-}A\beta)]$ complexes were observed compared to that of $[Cu^{II}(A\beta16)]$. These are the reason why components **I** and **II** of the $[Cu^{II}(H6R\text{-}A\beta)]$ complexes were also studied by ^{13}C NMR. In general, Cu(II) effect on the ^{13}C NMR spectra of the H6R mutant and on the Aβ16 peptide[16] are similar (Supporting Information Figure S7). More precisely, binding of both His13 and His14 in component **I** (see

dx.doi.org/10.1021/ic201739n |*Inorg. Chem.* 2011, 50, 11192–11201

CD part) may induce the binding of the CO function in between the two His residues, as proposed by calculations.[37] However, such a binding do not change the impact of Cu(II) to the ^{13}C NMR spectra of H6R-Aβ compared to Aβ16. Indeed, coordination of CO function from His residues was previously detected in the Aβ16 case and attributed to equilibrium in solution between $\{-NH_2, CO (Asp1), 2N_{Im}\}$ and $\{-NH_2, CO (His), 2N_{Im}\}$.[16] The main differences observed on the CO and C_α regions at pH 8.6, where component **II** is predominant, are shown in Figure 5. Both the CO functions and C_α atoms from His13 and His 14 residues are more broadened in the case of the H6R mutant. However, broadening of the CO and C_α ^{13}C atoms from the Ala2 residue, previously attributed to coordination of the amidyl function from the Asp1−Ala2 peptide bond, is still observed. Thus, this suggests that the deprotonation of the Asp1−Ala2 peptide bond also occurs in the H6R mutant but in this latter case, it does not induce the binding of the adjacent CO function (from Ala2 to Glu3). Indeed, CO functions from His residues may principally be involved in Cu(II) binding.

DISCUSSION

1. Coordination Sites of Cu(II) in Components I−IV. The proposed equatorial Cu(II) binding sites in components **I**−**IV** are shown in Scheme 1. Component **I** has been proposed by several groups.[15−19] In this species, the Cu(II) center is bound via the terminal amine, two His residues and a CO function mainly originating from the Asp1−Ala2 peptide bond.

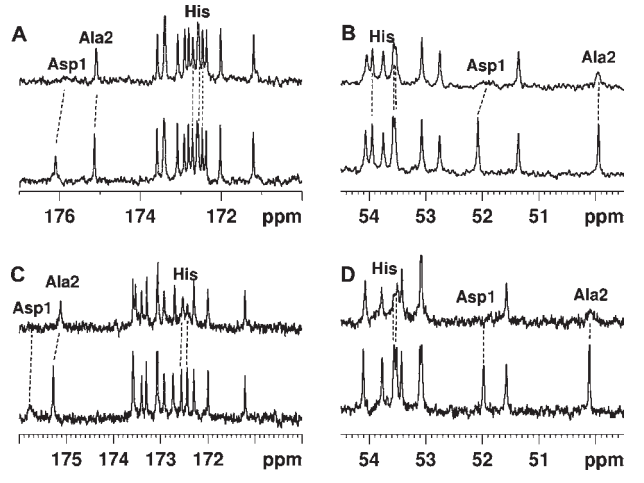

Figure 5. $^{13}C\{^1H\}$ NMR spectral regions of 10 mM Aβ16 peptide in D_2O (bottom spectra) and in presence of 0.1 equiv of Cu(II) (top spectra) at pH 8.7 (panels A and B) and of 5 mM H6R-Aβ peptide in D_2O (bottom spectra) and in presence of 0.05 equiv. of Cu(II) (top spectra) at pH 8.6 (panels C and D) T = 25 °C, ν = 125.8 MHz. Shift of some peaks is due to slight modification in the pH value induced by Cu(II) addition.

While consensus has been recently reached on Cu(II) coordination sphere in component **I**, this is not the case for component **II**. Indeed two models have principally appeared in the last years. In the first one, Cu(II) is bound via the carbonyl function from Ala2−Glu3 and the imidazole rings of the three His (model noted 1)[17,18] and in the second one, Cu(II) is bound via the terminal amine, the adjacent amide function from Asp1−Ala2, one out of the three His and the CO function from Ala2−Glu3 (model noted 2).[15,16] In the present study, new key insights have been obtained regarding the Cu(II) binding sphere in component **II**. First, an interesting feature is that Cu(II) complexes of the three H6A, H13A, and H14A mutants have EPR parameters identical to those of $[Cu^{II}(A\beta16)]$, indicating that the simultaneous equatorial coordination of the three His to the Cu(II) center is unlikely. Otherwise, this would imply that in complexes obtained with the His mutants, the His residues is replaced by a ligand that would influence the Cu(II) electronic properties in a very similar way, a possibility that we cannot however fully ruled out. Second, component **III** is identified as $\{-NH_2, 2N^-, N_{im}\}$ (see below) and thus it is difficult to rationalize why the terminal $-NH_2$ amine bound to Cu(II) in components **I** and **III**, will be unbound in the intermediate component **II**. Third, transition from components **I**−**II** (and to **III** and **IV**) is pH driven and thus should be concomitant to deprotonation of peptide function. In case of model 1, all the residues that can undergo deprotonation (i.e., the three His residues) are already deprotonated at pH below the pK_a(**I**/**II**) value and hence this model fails to explain the effect of pH in transition from **I** to **II**. Fourthly, contrarily to model 2, model 1 does not explain the variation in the pK_a(**I**/**II**) and pK_a(**II**/**III**) observed in $[Cu^{II}(D1N\text{-}A\beta)]$ and $[Cu^{II}(E3Q\text{-}A\beta)]$ complexes, respectively (see below). Fifthly, intervention of CO from Ala2−Glu3 preferentially to that of another peptide bond remains unexplained in model 1 whereas the deprotonation of the adjacent Asp1−Ala2 amide bond in model 2 justifies the intervention of the Ala2−Glu3 CO function in Cu(II) binding. Lastly, the EPR parameters of the very simple $[Cu^{II}(GGGGH)]$ complex (see Table 1), containing only one His residues in its sequence, are virtually identical to those found here for components **II**−**IV**, indicating that only one His can be bound to Cu(II) in components **II** and **III**.[29]

Regarding component **III**, EPR parameters, as well as NMR data support an "ATCUN" type Cu(II) site $\{-NH_2, 2N^-, Nim\}$. A $\{-NH_2, 3N^-\}$ Cu(II) equatorial site is proposed for component **IV** based on the EPR parameters and the difference with EPR signature of $[Cu^{II}(Ac\text{-}A\beta)]$. These propositions are in line with those previously reported by Kowalik et al. in their pioneer work,[21] except for component **IV** that was identified as $\{-N_{im}, 3N^-\}$. Moreover, in the present study attribution of each equatorial binding atoms has been proposed, that is, **I** = $\{-NH_2$, CO

Scheme 1. Proposed Equatorial Cu(II) Binding Sites of $[Cu^{II}(A\beta)]$ as a Function of pH

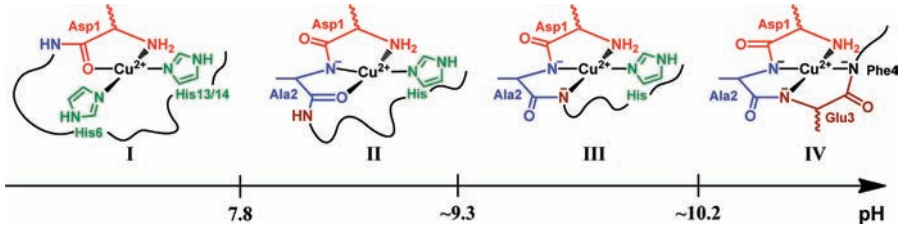

Scheme 2. D1N Mutation Decreases the pKa(I/II) Value by Precluding the $COO^- \cdots H-N$ (Asp1−Ala2) Interaction (7-Membered Metallacycle) while the E3Q Mutation Decreases the pKa(II/III) Value by Precluding the $COO^- \cdots H-N$ (Ala2−Glu3) Interaction (7-Membered Metallacycle)

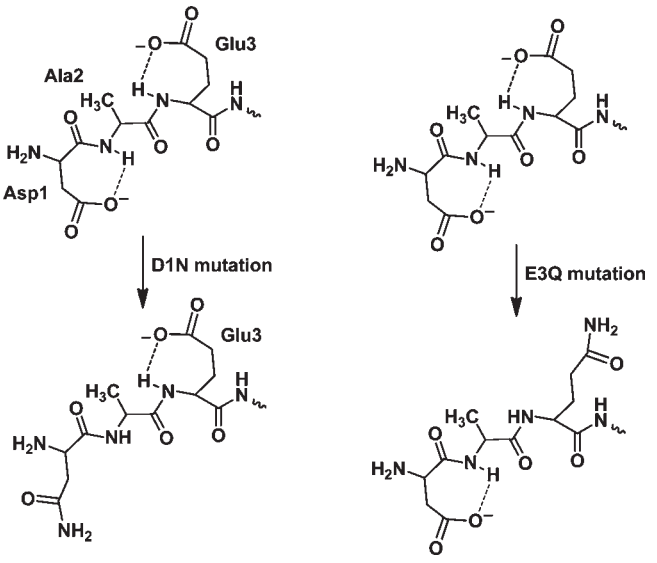

(Asp1−Ala2), N_{im} (His6), N_{im} (His13 or His14)}, **II** = {$-NH_2$, N^- (Asp1−Ala2), CO (Ala2−Glu3), N_{im}}, **III** = {$-NH_2$, N^- (Asp1−Ala2), N^- (Ala2−Glu3), N_{im}}, and **IV** = {$-NH_2$, N^- (Asp1−Ala2), N^- (Ala2−Glu3), N^- (Glu3−Phe4)}

Regarding involvement of carboxylate groups in Cu(II) apical position, the CD data obtained are in line with previous propositions that suggest a preferential role of the Asp1 residue.[15,16,18] Implication of the Glu3, Asp7, and Glu11 carboxylate groups in equilibrium with the one of Asp1 was also suggested for component **I**.[16] The CD data obtained here agree with this possibility except for the Glu11 residue, for the involvement of which no evidence was found.

D1N and E3Q mutations induced change in pK_a values between **I**/**II** and **II**/**III**, respectively (Table 1). More precisely, D1N mutation decrease the pK_a(**I**/**II**) value by more than one pH unit and the E3Q mutation decrease the pK_a (**II**/**III**) by more than 0.5 pH unit (Table 1). As previously pointed out,[33] this may be related to the breakage of H-bond network when carboxylate functions are modified to amide and subsequent easier deprotonation of peptide functions, here identified as the Asp1−Ala2 and Ala2−Glu3 peptide bonds, respectively. This is illustrated in Scheme 2, where the interventions of Asp1 and Glu3 are exemplified on the basis of model 2 for component **II**.

2. Coordination of Cu(II) to the H6R and D7N Familial Mutants. Among the various mutants studied here, Cu(II) coordination to the two H6R and D7N familial mutants linked to early onset of AD were investigated. While, regarding to Cu(II) coordination, the D7N mutation have no significant impact, the [Cu^{II}(H6R-Aβ)] complexes show differences with [Cu^{II}(Aβ16)]. More precisely, the pK_a(**I**/**II**) is significantly lower (about 0.5 pH unit) in the former case than in the latter, implying that at physiological pH the two components **I** and **II** will be differently distributed. More importantly, Cu(II) is differently bound in both components **I** and **II** of [Cu^{II}(H6R-Aβ)] and [Cu^{II}(Aβ)]. Proposed Cu(II) equatorial binding sites of [Cu^{II}(H6R-Aβ)] complexes are shown in Scheme 3. The most striking difference

Scheme 3. Proposed Equatorial Cu(II) Binding Sites of [Cu^{II}(H6R-Aβ)] as a Function of pH

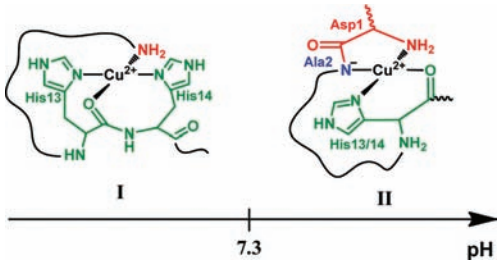

with [Cu^{II}(Aβ16)] is due to the concomitant involvement of His13 and His14 in Cu(II) binding in **I**, leading to outer first coordination shell effects observed by CD. Such equatorial binding of the His13-His14 diad (as minor form) in [Cu^{II}(Aβ16)] species compared to coordination of the His6 plus His13 or His14 (as major form) has been recently proposed to be linked to formation of amorphous aggregates.[20] In the [Cu^{II}(H6R-Aβ)] species, only the His13-His14 diad does intervene in Cu(II) equatorial binding in component **I**, and thus, the H6R mutation may be anticipated to be responsible of formation of only amorphous aggregates. In component **II**, intervention of CO from His13-His14 and His14-Gln15 peptide bonds in Cu(II) equatorial binding may also explained why component **III** is not detected in [Cu^{II}(H6R-Aβ)] complexes. Indeed, decoordination of the CO and the adjacent imidazole ring from His13 or His14 (forming a 6-membered metallacycle) residues may be concomitant, thus leading directly to a component **IV** (identical to the one obtained in case of the [Cu^{II}(Aβ)] species) from component **II**. Lastly, the [Cu^{II}(H6R-Aβ)] and [Cu^{II}(H6A-Aβ)] complexes have the same spectroscopical signatures implying that nature of the replacing residue in the H6 mutant is not a key factor.

CONCLUDING REMARKS

In the present paper, we reported the pH-dependent study of Cu(II) coordination to the Aβ peptide and to a series of mutants. While results obtained here are in perfect agreement with the Cu(II) equatorial binding site previously proposed in the literature for component **I** {$-NH_2$, CO (Asp1−Ala2), 2 N_{im}}, they also strongly supports a {$-NH_2$, N^-, CO (Ala2−Glu3), N_{im}} site in component **II**. Cu(II) complexes outside the physiological pH range have also been studied for expanding the number of spectroscopic references of Cu(II) peptidic species. Among the various mutants studied, the two familial H6R and D7N mutants were investigated and while the D7N mutation does not impact significantly Cu(II) coordination to Aβ, the H6R one leads to modification in Cu(II) binding that may also influence the peptide aggregating properties. During the course of these studies, the EPR and CD revealed to be complementary spectroscopies. Indeed, while EPR is a powerful technique to determine the Cu(II) equatorial environment, CD was very useful in disentangling effects outside the first coordination shell and for instance lead to the detection of a new species near pH 5.5.

EXPERIMENTAL SECTION

1. Sample Preparation. Studies were performed in H_2O or in D_2O. However, for clarity and consistency, we decided to use the notation pH even when the measurements were made in D_2O. pD was

dx.doi.org/10.1021/ic201739n |Inorg. Chem. 2011, 50, 11192–11201

measured using a classical glass electrode according to pD = $pH_{reading}$ + 0.4, and the pD value was adjusted according to ref 38 to be in ionization conditions equivalent to those in H_2O.

Aβ16 peptide (sequence DAEFRHDSGYEVHHQK and referred to as Aβ in the following), Ac-Aβ peptide corresponding to the N-terminally acetylated Aβ peptide, the D1N-Aβ (sequence NAEFRHDSGYEVHHQK), E3Q-Aβ (sequence DAQFRHDSGYEVHHQK), H6R-Aβ (sequence DAEFRRDSGYEVHHQK), H6A-Aβ (sequence DAEFRADSGYEVHHQK), D7N-Aβ (sequence DAEFRHNSGYEVHHQK), E11Q-Aβ (sequence DAEFRHDSGYQVHHQK), H13A-Aβ (sequence DAEFRHDSGYEVAHQK), H14A-Aβ (sequence DAEFRHDSGYEVHAQK), and the triple E3QD7NE11Q-Aβ C-terminally protected Aβ peptide (sequence DAQFRHNSGYQVHHQK-NH_2) were bought from GeneCust (Dudelange, Luxembourg) with purity grade >98%.

Stock solutions of peptide were prepared by dissolving the powder in Milli-Q water or in D_2O (resulting pH ~2). Peptide concentration was then determined by UV−visible absorption of Tyr10 considered as free tyrosine ($(\varepsilon_{276}$- $\varepsilon_{296}) = 1410\ M^{-1}cm^{-1}$) and the solution was diluted down to the appropriate concentration in peptide.

pH was adjusted using NaOH/HCl (H_2O) or NaOD/DCl (D_2O). All pH values are given with a ± 0.2 pH unit error.

a. Circular Dicroism (CD) Samples. Stock solution of peptide was diluted down to 0.5 mM in pure Milli-Q water; 0.9 equiv of Cu^{II} was added from 0.1 M $Cu(SO_4)$ stock solution.

b. Electron Paramagnetic Resonance (EPR) Samples. Stock solution of peptide was diluted down to 1.0 mM in D_2O; 0.9 equivalent of $^{63}Cu^{II}$ was added from 0.1 M $^{63}Cu(NO_3)_2$ stock solution. Samples were frozen in quartz tube, with addition of 10% glycerol as a cryoprotectant.

c. Nuclear Magnetic Resonance (NMR) Samples. Stock solution of H6R-Aβ peptide was diluted to about 5 mM in D_2O. Substoichiometric quantity (~0.05 equiv) of Cu^{II} from $Cu(SO_4)$ in D_2O was added. Cu^{II} to H6R-Aβ ratio was reduced to a minimum in the free peptide solution by working at 10 mM peptide concentration without buffer that is the primary source of paramagnetic contamination. Indeed a too high Cu^{II} to Aβ ratio would induce an uncontrolled broadening of NMR signals, a problem that may contributes to the loss of signals in the apo-peptide solution in previous studies.[39,40] Substoichiometric Cu^{II} ratio (0.05 equiv of Cu^{II} per Aβ peptide) was used. Indeed, this ratio is large enough to induce selective broadening of specific residues of all the peptides present in solution (because of fast exchange of Cu^{II} between peptides).

2. Spectroscopic Measurements. *a. Circular Dichroism (CD).* CD spectra were recorded on a JASCO circular dichroism spectrometer at 20 °C. Data were collected with a 1 nm sampling interval and 2 scans were averaged and a baseline spectrum was subtracted for each spectrum.

b. Electron Paramagnetic Resonance (EPR). EPR data were recorded using an Elexsys E 500 Bruker spectrometer, operating at a microwave frequency of approximately 9.5 GHz. All spectra were recorded using a microwave power of 20 mW across a sweep width of 150 mT (centered at 310 mT) with a modulation amplitude of 0.5 mT. Experiments were carried out at 110 K using a liquid nitrogen cryostat.

c. Nuclear Magnetic Resonance (RNMR). 1D ^1H and ^{13}C experiments and 2D experiments were recorded on a Bruker Avance 500 spectrometer equipped with a 5 mm triple resonance inverse Z-gradient probe (TBI ^1H, ^{31}P, BB) and a Bruker Avance 600 spectrometer equipped with a 5 mm triple resonance inverse (TCI ^1H, ^{13}C, ^{15}N) Z-gradient cryoprobe, respectively. All chemical shifts are relative to tetramethylsilane. 1D-NMR and 2D-NMR spectra were collected at 298 and 288 K in pure D_2O, respectively. Accumulation lasts c.a. Sixteen hours for the $^{13}C\{1H\}$ NMR experiments and 24 h for the 2D $^1H-^1H$ TOCSY, $^1H-^{13}C$ HSQC, and $^1H-^{13}C$ HMBC experiments.

All the ^1H and ^{13}C signals were assigned on the basis of chemical shifts, spin−spin coupling constants, splitting patterns and signal intensities, and by using $^1H-^1H$ TOCSY, $^1H-^{13}C$ HSQC, and $^1H-^{13}C$ HMBC experiments.

■ ASSOCIATED CONTENT

Ⓢ Supporting Information. pH-dependent EPR and CD spectra of [Cu^{II}(peptide] complexes, ^{13}C NMR spectra of H6R-Aβ, and assignments of the ^1H and ^{13}C signals of the H6R-Aβ peptide. This material is available free of charge via the Internet at http://pubs.acs.org.

■ AUTHOR INFORMATION

Corresponding Author

*E-mail: christelle.hureau@lcc-toulouse.fr. Phone: (+33) 5 61 33 31 62. Fax: (+33) 5 61 55 30 03.

Author Contributions

†These authors contributed equally to this work.

■ ACKNOWLEDGMENT

Authors thank the ANR (Agence Nationale de la Recherche), ANR Grant Neurometals NT09-488591. We thank Dr. L. Frémond for earlier results obtained on Cu(II) binding to H13A-Aβ and H14A-Aβ, Drs. L. Sabater, G. La Penna and P. Dorlet for fruitful discussions. Charles-Louis Serpentini is acknowledged for its participation in recording the CD data.

■ REFERENCES

(1) Holtzman, D. M.; Morris, J. C.; Goate, A. M. *Sci. Transl. Med.* **2011**, *3*, 77sr1.
(2) Castellani, R. J.; Smith, M. A. *J. Pathol.* **2011**, *224*, 147–152.
(3) Hardy, J.; Selkoe, D. J. *Science* **2002**, *298*, 789–791.
(4) Maccioni, R. B.; Muñoz, J. P.; Barbeito, L. *Arch. Med. Res.* **2001**, *32*, 367–381.
(5) Simón, A. M.; Frechilla, D.; del Rio, J. *Rev. Neurol.* **2010**, *50*, 667–675.
(6) Cappai, R.; Barnham, K. J. *Neurochem. Res.* **2008**, *33*, 526–532.
(7) Adlard, P. A.; Bush, A. I. *J. Alzheimer Dis.* **2006**, *10*, 145–163.
(8) Bush, A. I. *Trends Neurosci.* **2003**, *26*, 207–214.
(9) Cuajungco, M. P.; Faget, K. Y. *Brain Res. Rev.* **2003**, *41*, 44–56.
(10) Faller, P.; Hureau, C. *Dalton Trans.* **2009**, 1080–1094.
(11) Hureau, C.; Faller, P. *Biochimie* **2009**, *91*, 1212–1217.
(12) Kozlowski, H.; Janicka-Klos, A.; Brasun, J.; Gaggelli, E.; Valensin, D.; Valensin, G. *Coord. Chem. Rev.* **2009**, *253*, 2665–2685.
(13) Molina-Holgado, F.; Hider, R. C.; Gaeta, A.; Williams, R.; Francis, P. *Biometals* **2007**, *20*, 639–654.
(14) Smith, D. G.; Cappai, R.; Barnham, K. J. *Biochim. Biophys. Acta* **2007**, *1768*, 1976–1990.
(15) Dorlet, P.; Gambarelli, S.; Faller, P.; Hureau, C. *Angew. Chem., Int. Ed.* **2009**, *48*, 9273–9276.
(16) Hureau, C.; Coppel, Y.; Dorlet, P.; Solari, P. L.; Sayen, S.; Guillon, E.; Sabater, L.; Faller, P. *Angew. Chem., Int. Ed.* **2009**, *48*, 9522–9525.
(17) Drew, S. C.; Noble, C. J.; Masters, C. L.; Hanson, G. R.; Barnham, K. J. *J. Am. Chem. Soc.* **2009**, *131*, 1195–1207.
(18) Drew, S. C.; Masters, C. L.; Barnham, K. J. *J. Am. Chem. Soc.* **2009**, *131*, 8760–8761.
(19) Drew, S. C.; Barnham, K. J. *Acc. Chem. Res.* **2011**, DOI: 10.1021/ar200014u.
(20) Shin, B.-k.; Saxena, S. *J. Phys. Chem. A* **2011**, *115*, 9590–9602.
(21) Kowalik-Jankowska, T.; Ruta, M.; Wisniewska, K.; Lankiewicz, L. *J. Inorg. Biochem.* **2003**, *95*, 270–282.
(22) Kozlowski, H.; Bal, W.; Dyba, M.; Kowalik-Jankowska, T. *Coord. Chem. Rev.* **1999**, *184*, 319–346.
(23) Ono, K.; Condron, M. M.; Teplow, D. B. *J. Biol. Chem.* **2010**, *285*, 23186–23197.

(24) Hori, Y.; Hashimoto, T.; Wakutani, Y.; Urakami, K.; Nakashima, K.; Condron, M. M.; Tsubuki, S.; Saido, T. C.; Teplow, D. B.; Iwatsubo, T. *J. Biol. Chem.* **2007**, *282*, 4916–4923.
(25) Karr, J. W.; Kaupp, L. J.; Szalai, V. A. *J. Am. Chem. Soc.* **2004**, *126*, 13534–13538.
(26) Minicozzi, V.; Stellato, F.; Comai, M.; Dalla Serra, M.; Potrich, C.; Meyer-Klaucke, W.; Morante, S. *J. Biol. Chem.* **2008**, *283*, 10784–10792.
(27) Syme, C. D.; Nadal, R. C.; Rigby, S. E.; Viles, J. H. *J. Biol. Chem.* **2004**, *279*, 18169–18177.
(28) Hureau, C.; Eury, H.; Guillot, R.; Bijani, C.; Sayen, S.; Solari, P. L.; Guillon, E.; Faller, P.; Dorlet, P. *Chem.—Eur. J.* **2011**, *17*, 10151–10160.
(29) Várnagy, K.; Szabó, J.; Sóvágó, I.; Malandrinos, G.; Nick, H.; Sanna, D.; Micera, G. *J. Chem. Soc., Dalton Trans.* **2000**, 467–472.
(30) Hureau, C.; Charlet, L.; Dorlet, P.; Gonnet, F.; Spadini, L.; Anxolabéhère-Mallart, E.; Girerd, J.-J. *J. Biol. Inorg. Chem.* **2006**, *11*, 735–744.
(31) Peisach, J.; Blumberg, W. E. *Arch. Biochem. Biophys.* **1974**, *165*, 691–708.
(32) Eury, H.; Bijani, C.; Faller, P.; Hureau, C. *Angew. Chem., Int. Ed.* **2011**, *50*, 901–905.
(33) Karr, J. W.; Szalai, V. A. *J. Am. Chem. Soc.* **2007**, *129*, 3796–3797.
(34) Sarell, C. J.; Syme, C. D.; Rigby, S. E.; Viles, J. H. *Biochemistry* **2009**, *48*, 4388–4402.
(35) Rasia, R. M.; Bertoncini, C. W.; Marsh, D.; Hoyer, W.; Cherny, D.; Zweckstetter, M.; Griesinger, C.; Jovin, T. M.; Fernández, C. O. *Proc. Natl. Acad. Sci. U.S.A.* **2005**, *102*, 4294–4299.
(36) Gaggelli, E.; Bernardi, F.; Molteni, E.; Pogni, R.; Valensin, D.; Valensin, G.; Remelli, M.; Luczkowski, M.; Kozlowski, H. *J. Am. Chem. Soc.* **2005**, *127*, 996–1006.
(37) Raffa, D. F.; Gómez-Balderas, R.; Brunelle, F.; Rickard, G. A.; Rauk, A. *J. Biol. Inorg. Chem.* **2005**, *10*, 887–903.
(38) Delgado, R.; Da Silva, J. J. R. F.; Amorim, M. T. S.; Cabral, M. F.; Chaves, S.; Costa, J. *Anal. Chim. Acta* **1991**, *245*, 271–282.
(39) Danielsson, J.; Pierattelli, R.; Banci, L.; Graslund, A. *FEBS J.* **2007**, *274*, 46–59.
(40) Hou, L.; Zagorski, M. G. *J. Am. Chem. Soc.* **2006**, *128*, 9260–9261.